Three-dimensional micro-Raman spectroscopy mapping of stress induced in Si by Cu-filled through-Si vias

Daisuke Kosemura and Ingrid De Wolf

Citation: Applied Physics Letters **106**, 191901 (2015); doi: 10.1063/1.4921004
View online: http://dx.doi.org/10.1063/1.4921004
View Table of Contents: http://scitation.aip.org/content/aip/journal/apl/106/19?ver=pdfcov
Published by the AIP Publishing

Three-dimensional micro-Raman spectroscopy mapping of stress induced in Si by Cu-filled through-Si vias

Daisuke Kosemura[a] and Ingrid De Wolf[b]
imec, Kapeldreef 75, 3001 Leuven, Belgium

(Received 17 February 2015; accepted 29 April 2015; published online 11 May 2015)

Three-dimensional (3D) micro-Raman spectroscopy mapping of mechanical stress induced by Cu through-Si vias (TSVs) in the Si substrate is reported. The 3D-map is obtained by combining 2D-maps measured at different positions along the cross-section of TSVs. The results highlight the relaxing effect of cross-sectioning on the stress field and show that conventional 2D-measurements on cross-sections can seriously underestimate the real stress values. Using this technique, the impact of post-plating anneal on the TSV stress is measured and shown to correlate very well with TSV stress data obtained from wafer bending experiments. © *2015 AIP Publishing LLC*.
[http://dx.doi.org/10.1063/1.4921004]

In order to improve performance, functionality, and density of Si integrated circuits (Si-ICs), a lot of research is focusing on three-dimensional (3D)-stacked Si-IC technology. In this technology, thinned Si chips are stacked and electrically interconnected by through-Si vias (TSVs) and micro-bumps.[1,2] It is well known that Cu filled TSVs introduce mechanical stress in the Si.[3] This stress is a concern for reliability: Problems such as delamination,[4,5] stress-induced voiding,[6] TSV liner-barrier integrity,[7] and Cu pumping[8] were reported in the literature. Mechanical stress also changes the mobility of electrons and holes, through the piezo-electric effect in Si, and as such affects the transistor characteristics.[9] Due to this problem, a transistor "keep-out" zone is defined around the TSV. This keep-out zone (KOZ) not only depends on transistor type and technology node[10,11] but also depends highly on the TSV processing conditions.[12]

All these concerns underline the importance to accurately measure the TSV induced-stress in the Si in order to understand its origin and to investigate the effect of TSV dimensions and processing parameters on the stress values.

Micro-Raman spectroscopy (μRS) is often used to study the stress imposed by TSVs in the surrounding Si.[13–17] The measurements are, in general, performed from the top surface: The Raman spectra of Si are measured during a line or 2D scan across the surface and the shift of the Raman peak frequency ($\Delta\omega$) from the stress value is plotted. This provides information on the stress near the Si surface, which is relevant for its impact on nearby transistors, but only gives limited information of the stress field near a TSV. Often in-plane stress is assumed, but it was demonstrated that μRS measurements from the top surface can be highly affected by the compressive axial component, which is of less relevance for the KOZ.[13]

Measurements from the cross-section are expected to provide a more complete picture and are required to understand the exact origin and sources of TSV stresses. There are very few reports of such measurements. In Ref. 13, it was shown that dominating compressive stress is present in the bulk Si near 5 μm diameter, 50 μm deep TSVs, and dominating tensile stress near the TSV bottom. In Ref. 14, the impact of temperature on TSV-induced stress was demonstrated using μRS on cross-sections made through $30 \times 30\,\mu m^2$ square, 100 μm deep TSVs. In both papers, the cross-sections were made through the center of the TSVs.

In this letter, we demonstrate 3D-μRS mapping on the cross-section of TSVs. The results highlight the relaxing effect of cross-sectioning on the stress field and show that conventional 2D-measurements on cross-sections can seriously underestimate the real stress values. Using this technique, the impact of post-plating anneal on the TSV stress is measured and shown to correlate very well with TSV stress data obtained from wafer bow experiments.

Measurements were performed on samples with 10 μm diameter/100 μm deep Cu-filled TSVs. The stress in the TSVs in these samples was estimated using a combination of wafer bow measurements and finite element models, as discussed in Ref. 12. This resulted in the average in-plane (radial) stress within the TSVs in function of the post-plating anneal temperature, as shown in Fig. 1. Three of these

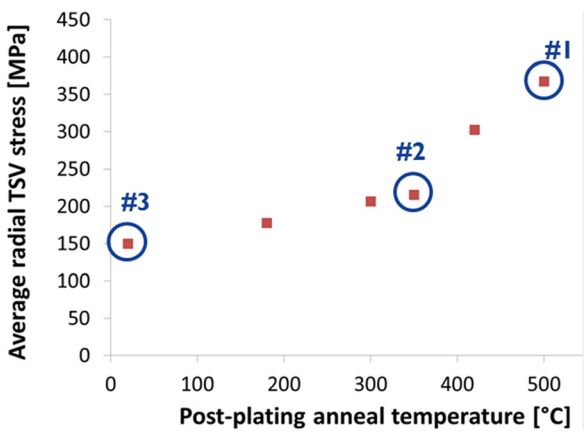

FIG. 1. Average radial TSV stress as a function of post-plating anneal temperature.

[a]Electronic addresses: daisuke.kosemura@imec.be and ingrid.dewolf@imec.be
[b]Also at Department Materials Engineering, Faculty of Engineering, KU Leuven, 3001 Leuven, Belgium.

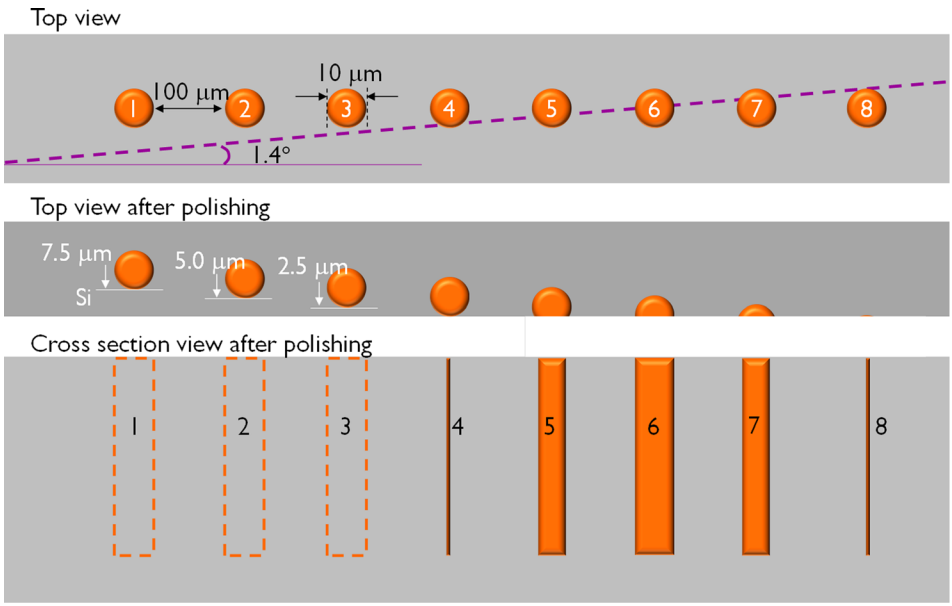

FIG. 2. Cross-sections at different positions with regard to the TSVs obtained by mechanical polishing under an angle of 1.4°.

samples, indicated by circles in Fig. 1, were selected for the current μRS experiments: sample #1 with high radial stress (500 °C post-plating anneal), sample #2 with medium stress (350 °C post-plating anneal), and sample #3 with low stress (room temperature, no post-plating anneal).

Samples for cross-sectional μRS measurements are, in general, fabricated by polishing parallel to the chip edge until the center of the structure to be investigated is reached. However, in case of a circular TSV, this process takes away half of the TSV, so a large part of the stress source. In addition, the free cross-section surface can relax resulting also in stress decrease. To avoid this problem, samples containing an array of TSVs were mechanically polished under an angle of 1.4°. This resulted in cross-sections at different positions with regard to the TSV (Fig. 2). The distance between each cross-section is ~2.5 μm. In some cross-sections, the TSV is still fully embedded in the Si (nos. 1, 2, and 3). In cross-section no. 4, the TSV is just touched. Cross-section no. 6 is the conventional one through the center of the TSV. By adapting the angle or using different pitches of the TSVs, more or less cross-section positions can be obtained. One can assume that all these TSVs, having seen the same process conditions and being on the same chip, have the same stress. As such, this sample can be used to measure μRS data at different cross-section positions through the TSVs. Another method could be to cross-section until position 1, measure the Raman spectra, cross-section further, measure again, etc. This approach would be much more cumbersome and time consuming.

μRS measurements were done in backscattering geometry from the $(1\ \bar{1}\ 0)$ cross-section plane using the 633 nm excitation wavelength. For this wavelength, the probing depth is approximately 3 μm. This is calculated using the methodology proposed by Ref. 18 and the optical absorption coefficient data from Ref. 19. Measurements were only done for one polarization of the incident laser light, i.e., parallel to the length of TSVs.

Fig. 3 (top) shows optical microscopy images of sample #1 (500 °C post-plating anneal) after polishing along an angle, as explained in Fig. 2. First line-scan μRS experiments were performed on the cross-section at a depth of 50 μm under the Si surface, as indicated in Fig. 3. The Si-Raman peak was fitted using a Lorentz function and the measured frequency shift from the stress free value is plotted under the relative cross-section pictures. Cross-section no. 6 of this sample corresponds with the traditionally investigated cross-section, i.e., right through the center of the TSV. Only a very small Raman frequency shift is measured here. This would lead to the conclusion that the stress near this TSV is very small. However, when doing the same measurement at non-standard cross-section positions, much higher Raman frequency shifts are detected. In cross-section no. 1, where the full TSV is still present and covered by 7.5 μm Si, a clear positive Raman frequency shift of about 0.3 cm^{-1} is measured.

This positive shift meaning compressive stress originates mainly from the circumferential stress component, which is confined close to the TSV.[13] The direction of the circumferential stress component in front of the TSV is parallel to the cross-section, while, at both (left and right) sides of the TSV, it is perpendicular to the cross-section, which is partly relaxed at the cross-section. That is why this compressive stress rapidly decreases with respect to the distance at the sides of the TSV, as is visible in Fig. 3.

In cross-sections 2, 3, and 4, approaching the TSV, this shift becomes larger, up to 1.7 cm^{-1} close to the TSV in cross-section 4, and a tensile stress field is observed in the Si at a larger distance from the TSV. It is clear that by taking away the Cu by further polishing, also the stress drops very fast. This shows that a study of a cross-section such as no. 4 provides more information than the traditional half-TSV cross-section no. 6.

To obtain information on the stress field around the complete TSV, Si-Raman spectra were measured in 2D regions on cross-sections 1–8. The measured Raman frequency shifts are shown in Fig. 4(a). Actually, the combination of these 2D results provides a 3D-μRS image of the stress field near the TSV, as shown in Fig. 4(b). These results clearly demonstrate the stress field around the TSV and how this field changes with polishing. These data contain much more information on the stress field near a TSV than can be

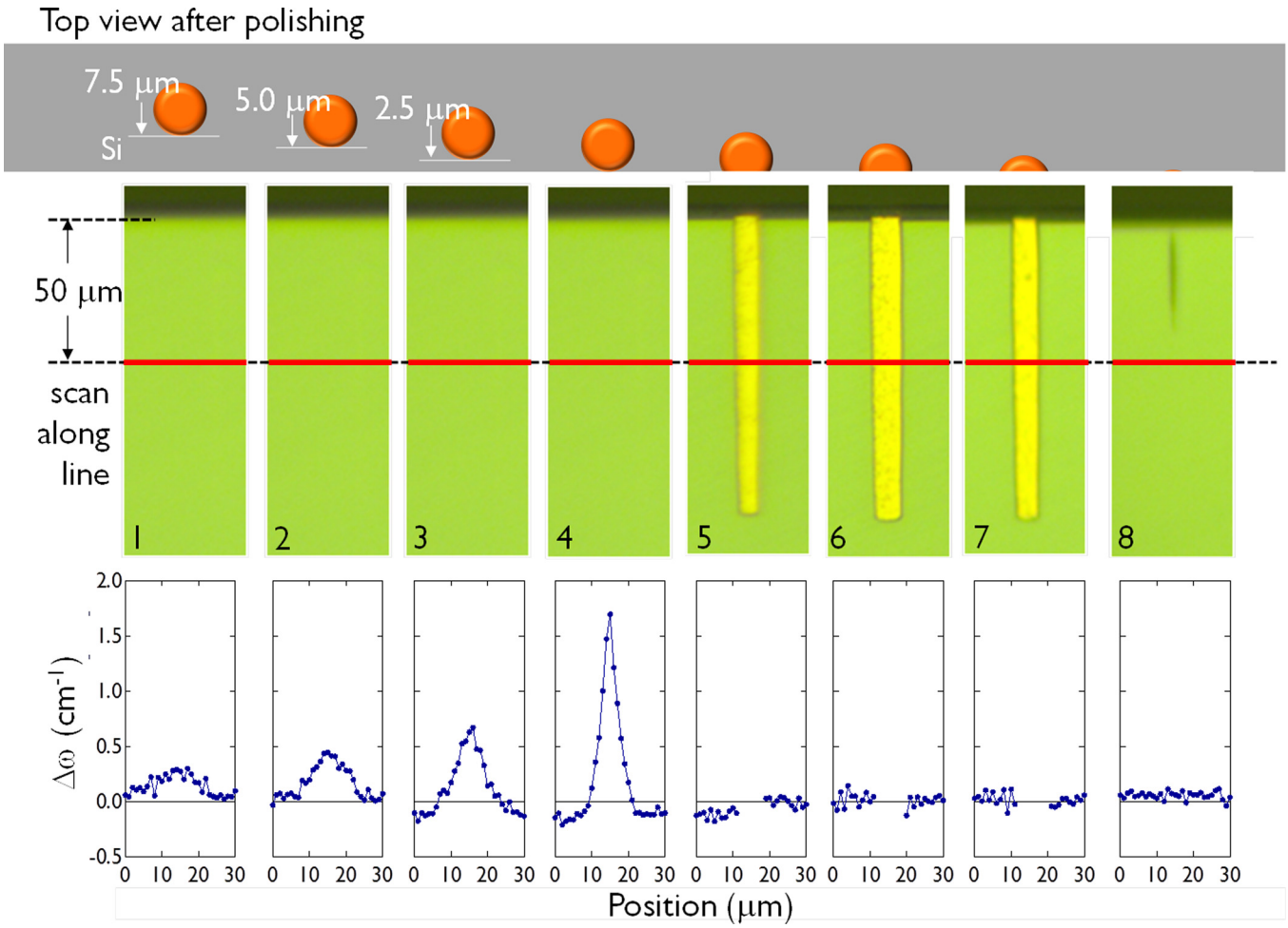

FIG. 3. Optical microscope images of sample #1 after polishing along an angle of 1.4° and results of the line-scan μRS experiments performed on the cross-section at a depth of 50 μm under the top surface.

obtained from a single cross-section analysis through the center of a TSV.

These results show a cross-sectional measurement of stress near a TSV that is still fully embedded in silicon (cross-sections 1, 2, and 3). A clear positive Raman frequency shift (blue) in the Si in front of the TSV is observed. This indicates that the compressive axial and circumferential stress components dominate at this position.[1] The results also confirm that there is not only stress near the surface of the TSV as often assumed but also along the full length.[13,14] The measured positive Raman frequency shift increases when measuring closer to the TSV and can become very high, even up to 1.7 cm^{-1} (see Fig. 3, no. 4).

When assuming for simplicity uniaxial stress along the surface (x: [110] direction), the relation between that stress, σ_{xx}, and the Raman frequency shift ($\Delta\omega_1$) is given by[14]

$$\Delta\omega_1(\mathrm{cm}^{-1}) = -2.88 \times \sigma_{xx}(\mathrm{GPa}). \quad (1)$$

To obtain the coefficient, we used the elastic compliance constants S_{11}, S_{12}, and S_{44} and phonon deformation potentials p, q, and r in Refs. 20 and 21, respectively. This would correspond with stresses in the order of 600 MPa. This is much higher than obtained from surface measurements or predicted from FEM calculations: they predict stresses in the range of 200 MPa. This high value can be explained by the fact that the TSV induced stress acts on a very thin slice of Si at this position, which is not confined anymore by the Si bulk. To understand this further, one can assume that Si is consisting of several thin layers. If many layers are present, the strain imposed by the Cu is taken by all layers, in a gradual way (higher strain in layers close to the Cu). When only one layer is present, this layer has to take all the strain, and as a result the strain in the first layer will be higher than if many layers are present.

Near the top surface, a clear tensile stress field is detected, indicating that the radial tensile stress component dominates, which is difficult to be detected by the Raman measurements from the top-surface, as described in Ref. 13, because in backscattering measurements from the top surface, the radial and circumferential stress have equal but opposite effect on the Raman peak position. For this reason, in such experiments the effect of the axial compressive stress will dominate the measured Raman frequency shift. Also in the bulk but further away from the TSV, tensile stress is detected which becomes very clear in cross-section no. 4. This fits with the theory that the tensile radial stress extends further from the TSV than the compressive stress.[13] In addition, by removing the front Si, the circumferential stress next to the TSV is expected to decrease, and as a result the radial tensile stress becomes more dominating in the Raman data. For cross-section no. 5, the radial tensile stress field seems to be asymmetric, as shown in Figs. 3 and 4. This is because

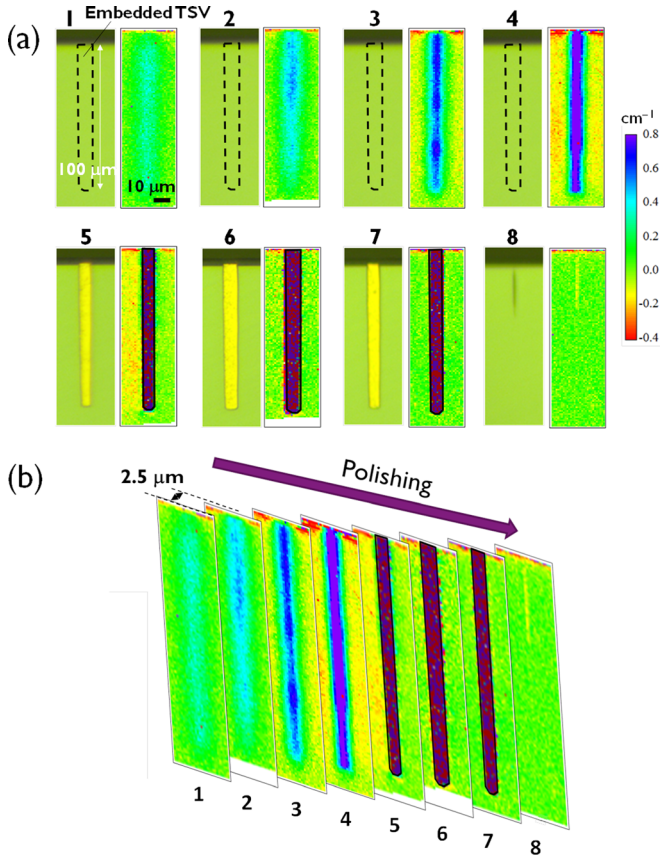

FIG. 4. (a) 2D Raman frequency shifts on cross-sections 1 to 8. (b) Same images as shown in (a), combined into a 3D-μRS image.

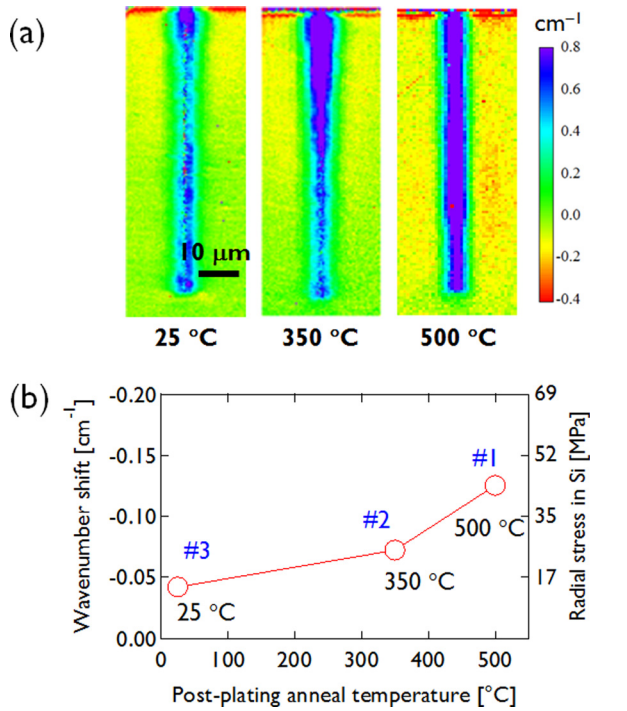

FIG. 5. (a) 2D Raman frequency shifts on cross-sections of samples #1, #2, and #3. (b) Left axis: The average value of the negative Raman frequency shift (tensile stress) measured at a depth of 50 μm in the cross-section as a function of post-plating anneal temperature. Right axis: The calculated stress value assuming out-of-plane and axial stress to be zero (Eq. (1)).

the sample is asymmetric. Indeed, the left side of the TSV no. 5 is close to cross-section no. 4 where more tensile stress is measured, while the right side is closer to no. 6 showing less stress.

Stress near the TSV can be described by different stress components (axial, radial, circumferential, and shear), and by changing the cross-section, these components are affected in a different way, which also affects the measured Raman frequency shift.[13,14] These 3D-μRS data provide a lot of information on the stress near TSVs. The compressive stress in the Si in front of the TSV is not measured on a traditional cross-section but is clearly visible in these results. Also the tensile stress left and right of the TSV, not only at the surface but also in the bulk of the Si, is not captured with the traditional method. When combined with finite element models which take into account the cross-sectioning and the Raman spectroscopy parameters such as probing spot size and laser penetration depth, these 3D-μRS data will provide information on all stress tensor components and of the causes of this stress.

Similar measurements were performed on cross-sections of samples #2 (350 °C post-plating anneal) and #3 (no post-plating anneal). According to the wafer curvature measurements, the tensile stress in the TSVs is different for these samples, and so different stresses in the Si are expected. The measurement results obtained on cross-sections no. 4 are used to compare these samples (Fig. 5(a)). The results clearly indicate a decrease of the Raman frequency shift, and thus the stress, with decreasing post-plating anneal. Making this conclusion based on the results from cross-sections through the center of the TSV was not possible because of the noise in the data. However, using 3D-μRS data, i.e., results from different cross-sections, strengthens this conclusion. To compare these results with the ones presented in Fig. 1, the average value of the tensile stress at a depth of 50 μm in no. 4 (Fig. 5(a)) was calculated, and plotted in Fig. 5(b) as a function of the post-plating anneal temperature. The Raman frequency shift for these three samples shows the same trend as obtained from the wafer curvature measurements (Fig. 1), where the average radial stress in the TSV was calculated.[12]

From the wafer bow, only the radial stress in the Cu of the TSV is estimated. The measured Raman shifts depend on radial, axial, and circumferential stress. If we assume that on the cross-section the out-of-plane stress and the axial stress can be neglected, the radial stress can be calculated using Eq. (1). The result of this calculation is shown on the right axis of Fig. 5(b). However, the calculated value is stress in Si, which cannot directly be compared with the stress in Cu shown in Fig. 1. For a more detailed stress extraction of stress values from the Raman data, FEM is required. But the results confirm the validity and sensitivity of the measurements on these cross-sections. The wafer curvature experiments only give a mean value, while these 3D-μRS experiments show the local changes of the stress, along the full length of the TSV.

In this letter, we have demonstrated 3D-Raman spectroscopy mapping. This technique was applied to study the stress fields in Si around Cu-filled TSVs. It is shown that cross-sectioning results in a large stress relaxation, due to removing part of the stress source (the Cu-TSV) and due to surface relaxation. As such, performing measurements on only one cross-section (mostly through the mid of a TSV) provides

only limited information on the stresses and underestimates the stress values. It is shown that by using 3D-μRS, the effect of processing conditions, such as post-plating anneal, on the stress in TSVs can be studied in much better detail. 3D-μRS combined with FEM is believed to allow to deduce all stress tensor elements.

The authors thank Mario Gonzalez, Joke De Messemaeker, and Nabi Nabiollahi for samples and discussions, and Thomas Nuytten and Veerle Simons of imec for help with the instrumentation. This work was performed for the 3D program of imec, and the authors thank all imec contributors and industrial partners of this program. This study was partially supported by the JSPS Postdoctoral Fellowships for Research Abroad.

[1]*Handbook of 3D Integration*, edited by P. Garrou, C. Bower, and P. Ramm (Wiley-VCH Verlag GmbH & Co. KGaA, Weinheim, 2008).
[2]P. Marchal, B. Bougard, G. Katti, M. Stucchi, W. Dehaene, A. Papanikolaou, D. Verkest, B. Swinnen, and E. Beyne, Proc. IEEE **97**, 96 (2009).
[3]C. Okoro, Y. Yang, B. Vandevelde, B. Swinnen, D. Vandepitte, B. Verlinden, and I. De Wolf, in *Proceedings of the IEEE Interconnect Technology Conference, Burlingame, CA, USA* (2008), pp. 16–18.
[4]B. Debecker, K. Vanstreels, M. Gonzalez, B. Vandevelde, and Z. Tokei, in *IEEE International Conference on Thermal, Mechanical and Multi-Physics Simulation and Experiments in Microelectronics and Microsystems, Wroclaw, Poland* (2013), pp. 1–5.
[5]K. H. Lu, S.-K. Ryu, Q. Zhao, X. Zhang, J. Im, R. Huang, and P. S. Ho, in *Proceedings of the IEEE Electronic Components and Technology Conference, Las Vegas, USA* (2010), pp. 40–45.
[6]K. Croes, V. O. Cherman, Y. Li, L. Zhao, Y. Barbarin, J. De Messemaeker, Y. Civale, D. Velenis, M. Stucchi, T. Kauerauf, A. Redolfi, B. Dimcic, A. Ivankovic, G. Van der Plas, I. De Wolf, G. Beyer, B. Swinnen, Z. Tőkei, and E. Beyne, in *Proceedings of the IEEE Physical and Failure Analysis of Integrated Circuits, Singapore* (2012), pp. 1–5.
[7]Y. Li, S. Van Huylenbroeck, E. Van Besien, X. Shi, C. Wu, M. Stucchi, G. Beyer, E. Beyne, I. De Wolf, and K. Croes, Microelectron. Reliab. **54**, 1949 (2014).
[8]J. De Messemaeker, O. V. Pedreira, H. Philipsen, E. Beyne, I. De Wolf, T. Van der Donck, and K. Croes, in *Proceedings of the IEEE Electronic Components and Technology Conference, Orlando, USA* (2014), pp. 613–619.
[9]W. Guo, G. Van der Plas, A. Ivankovic, V. Cherman, G. Eneman, B. De Wachter, M. Togo, A. Redolfi, S. Kubicek, Y. Civale, T. Chiarella, B. Vandevelde, K. Croes, I. De Wolf, I. Debusschere, A. Mercha, A. Thean, G. Beyer, B. Swinnen, and E. Beyne, IEDM Tech. Dig. **2012**, 18.4.1–18.4.4.
[10]W. Guo, V. Moroz, G. Van der Plas, M. Choi, A. Redolfi, L. Smith, G. Eneman, S. Van Huylenbroeck, P. D. Su, A. Ivankovic, B. De Wachter, I. Debusschere, K. Croes, I. De Wolf, A. Mercha, G. Beyer, B. Swinnen, and E. Beyne, IEDM Tech. Dig. **2013**, 12.8.1–12.8.4.
[11]A. Mercha, G. Van der Plas, V. Moroz, I. De Wolf, P. Asimakopoulos, N. Minas, S. Domae, D. Perry, M. Choi, A. Redolfi, C. Okoro, Y. Yang, J. Van Olmen, S. Thangaraju, D. Sabuncuoglu Tezcan, P. Soussan, J. H. Cho, A. Yakovlev, P. Marchal, Y. Travaly, E. Beyne, S. Biesemans, and B. Swinnen, IEDM Tech. Dig. **2010**, 2.2.1–2.2.4.
[12]J. De Messemaeker, O. V. Pedreira, B. Vandevelde, H. Philipsen, I. De Wolf, E. Beyne, and K. Croes, in *Proceedings of the IEEE Electronic Components and Technology Conference, Las Vegas, USA* (2013), pp. 586–591.
[13]I. De Wolf, V. Simons, V. Cherman, R. Labie, B. Vandevelde, and E. Beyne, in *Proceedings of the IEEE Electronic Components and Technology Conference, San Diego, USA* (2012), pp. 331–337.
[14]R. Sugie, K. Kosaka, H. Seki, H. Hashimoto, and M. Yoshikawa, J. Appl. Phys. **114**, 233503 (2013).
[15]S.-K. Ryu, Q. Zhao, M. Hecker, H.-Y. Son, K.-Y. Byun, J. Im, P. S. Ho, and R. Huang, J. Appl. Phys. **111**, 063513 (2012).
[16]W. S. Kwon, D. T. Alastair, K. H. Teo, S. Gao, T. Ueda, T. Ishigaki, K. T. Kang, and W. S. Yoo, Appl. Phys. Lett. **98**, 232106 (2011).
[17]R. P. Koseski, W. A. Osborn, S. J. Stranick, F. W. DelRio, M. D. Vaudin, T. Dao, V. H. Adams, and R. F. Cook, J. Appl. Phys. **110**, 073517 (2011).
[18]J. Takahashi and T. Makino, J. Appl. Phys. **63**, 87 (1988).
[19]D. E. Aspnes and A. A. Studna, Phys. Rev. B **27**, 985 (1983).
[20]W. A. Brantley, J. Appl. Phys. **44**, 534 (1973).
[21]E. Anastassakis, A. Cantarero, and M. Cardona, Phys. Rev. B **41**, 7529 (1990).